Electronic Supplementary Information

Confinement effects in the hydrogen adsorption on paddle wheel containing metal-organic frameworks

Diego A. Gomez, Aldo F. Combariza, and German Sastre*

Instituto de Tecnología Química U.P.V.-C.S.I.C. Universidad Politécnica de Valencia, Avenida Los Naranjos s/n, 46022 Valencia, Spain. E-mail: *gsastre@itq.upv.es*

Table of Contents

S1. Computed physical properties and H_2 uptakes.

The computed accessible surface and the pore volume values calculated in this study for the MOFs in table 4 were compared with the experimental values reported in the literature (see Figure S1).

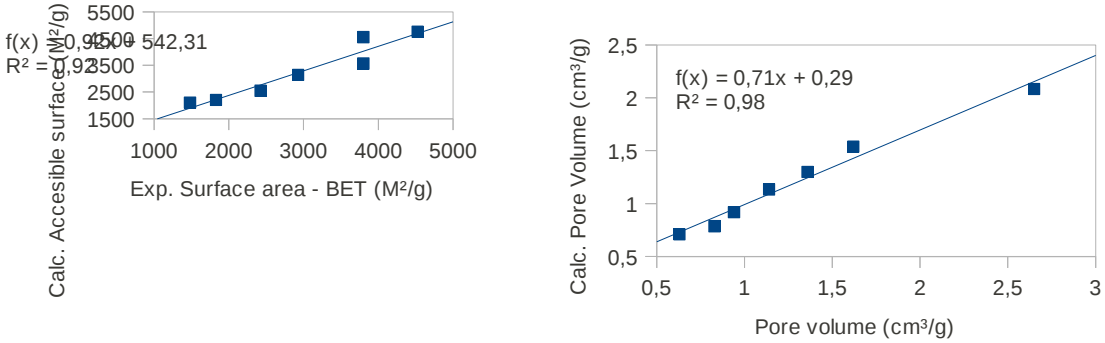

Figure S1. Comparison of the experimental and calculated surface area and pore volumes. The trend line, the fixed equation, and the correlation coefficient are shown.

The Figure S1 shows that both the accessible surfaces and the pore volumes computed in this study with the mentioned geometrical procedures are in close agreement with the experimental values reported in the literature.

On the other hand, the Figure S2 presents graphs of the experimental H_2 uptakes at low pressure and the computed physical properties of Table 4 (accessible surface, pore volume and metal atoms density).

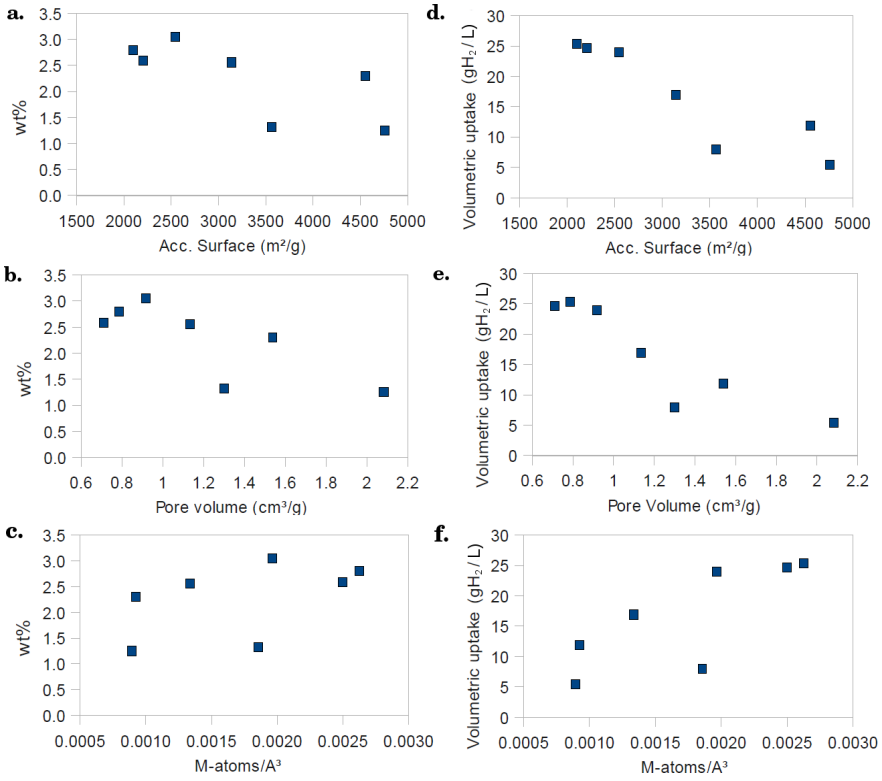

Figure S2. Gravimetric (a-c) and Volumetric (d-f) uptakes as a function of the computed values for accessible surface, metal atoms density and pore volume.

At first glance, the trends observed for the gravimetric and volumetric uptakes as a function of the accessible surface values (Figure S2, a and d) and the pore volumes (Figure S2, b and e) are similar. In general words, as bigger the value of the physical property, lower the value of the uptake obtained at 1 bar for the MOFs evaluated (see Table 4).

In the case of the accessible surface, this behaviour is explained by the fact that the surface area is tightly linked to the size of the organic ligands, therefore a high surface area does not indicate a high number of the strongest adsorption centres, which promote the adsorption at low pressures. Conversely, the mass relation between the H_2 adsorbed and the mass of the MOF is lower. As mentioned in the main manuscript, the organic ligands promote the formation of strong adsorption centres in small cavities which are not homogeneously distributed in the crystalline structure.

The relation of the gravimetric and volumetric uptake with the pore volume (Figure S2, b and e) is similar to the mentioned for the accessible surface. However, at low values of pore volume the graph suggest a maximum of the uptakes, for the paddle wheel containing MOFs, at pore volume of 0.9-1.0 cm^3/g. This result agree with the posed discussion about the effect of the framework topology and the confinement effects in the gas adsorption, which was rationalized in terms of pore size and the presence of small cavities.

Regarding to the relation of the gravimetric and volumetric uptakes with the metal atoms density (Figure S2, c and d), the graph suggest an increase of the uptake with the density of metal atoms. As mentioned,

the adsorption at low pressure is promoted by the strongest adsorption centres, therefore as larger the amount of accessible metal atoms per volume unit, larger adsorption is expected. In this case the limits will be imposed by the distance between the metal atoms (overlap of adsorption centres) and the relation between the adsorption strength and the intermolecular repulsion.

S2. Monte Carlo simulation and pressures.

The Monte Carlo (MC) simulations were performed to determine a reasonable starting configuration for an arbitrary number of molecules in the unit cell of each material. These arbitrary loadings were defined homogeneously for all the materials as the number of molecules required to occupy a third part of the pore volume of the material. For this estimation the volume of a H_2 molecule was approached to 47.12 $Å^3$ and the pore volume was estimated employing the PLATON code.

In order to take an idea on the range of pressures at which our simulations were performed, we compute the theoretical gravimetric uptake (wt% Theo.) and from the experimental adsorption isotherm reported for each material we estimate the corresponding pressure. The values obtained, reported in the following table, indicate that the MD simulations were performed at low pressures (0.3-2.0 bar) as expected, given that the purpose of the study was to identify the main adsorption centres promoted by interaction with the open metal sites and by confinement effects.

Table S1. Estimated gravimetric uptakes (wt% Theo.) at which MD simulations were performed and corresponding pressures (bar) obtained from extrapolation in the experimental adsorption isotherms.

	Wt (%) Theo.	Pressure (bar)
PCN-12	2.1	0.3
H-KUST-1	1.8	0.9
MOF-505	1.7	0.3
NOTT-103	2.6	0.8
NOTT-112	3.5	~2.0

S3. Cu···H_2 force field parameters tested.

In order to define a right set of force field parameters for the H_2···Cu-paddle wheel interaction, several values for the well depth of a Lennard-Jonnes (LJ) and Morse function were tested. Some occupancy maps obtained with the different potentials tested are presented in the Figure S3 and S4.

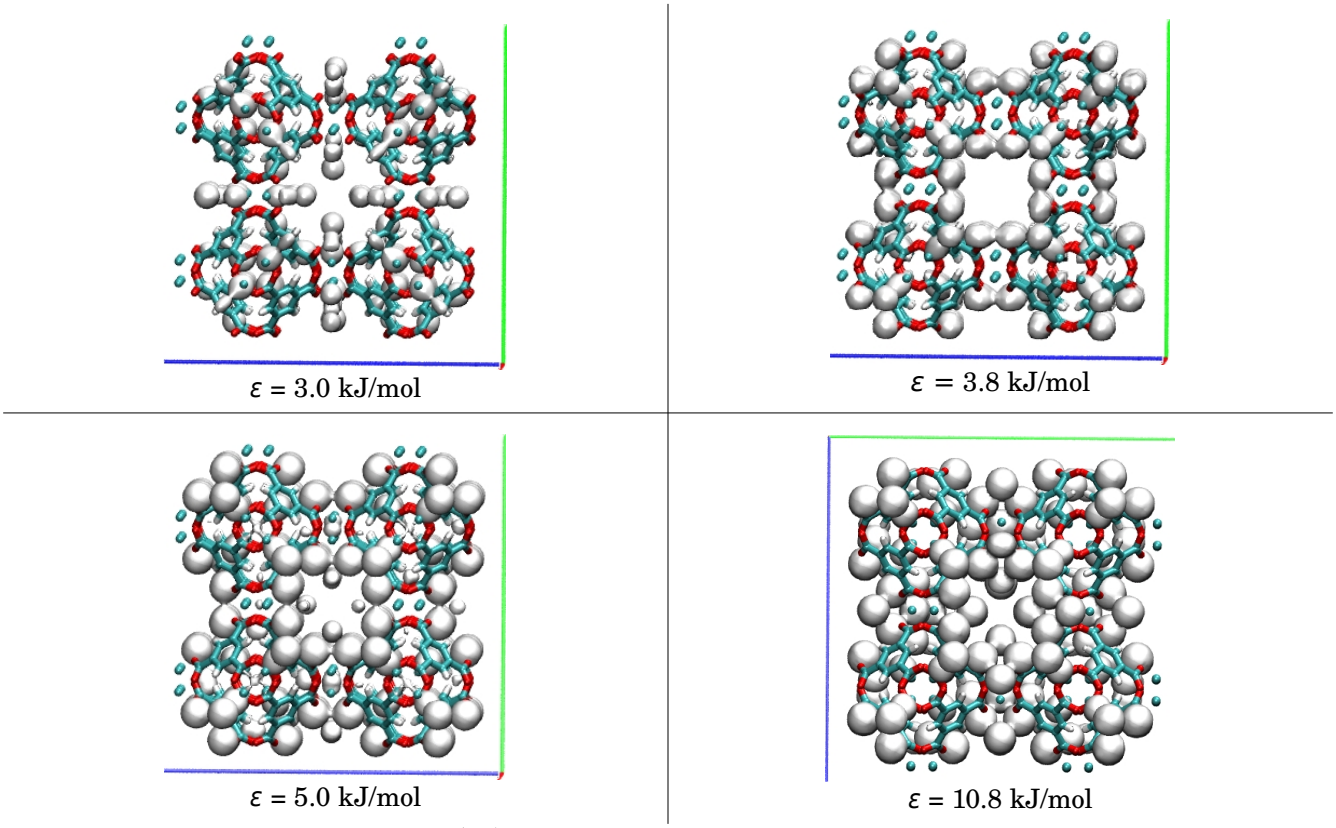

Figure S3. Occupancy maps with $O^{(x,y,z)}$=60% calculated from MD simulations with a LJ function for the H_2···Cu(II) interaction employing different values of 'ε'.

For values of 'ε' < 3.0 kJ/mol, the strongest adsorption position (labelled as P1 in the manuscript) was not observed in the occupancy maps. However, although with a value of 3.0 kJ/mol the occupancy map (with $O^{(x,y,z)}$=60%) is close to the INS report[1], some adsorption position into the biggest cavities at lower values of $O^{(x,y,z)}$ (<30%) are not in agreement with the experimental result. Additionally, a value of 3.0 kJ/mol for the Cu(II)···H_2 interaction represents a weaker interaction than the indicated by the experiments and the DFT calculations (see below).

On the other hand, the results obtained with the LJ function for the strongest interaction (-10.8 kJ/mol) gave an unclear definition of the adsorption positions due to the overlap of the adsorption regions. So the potential curvature was an additional parameter to test. This was done employing a Morse potential function.

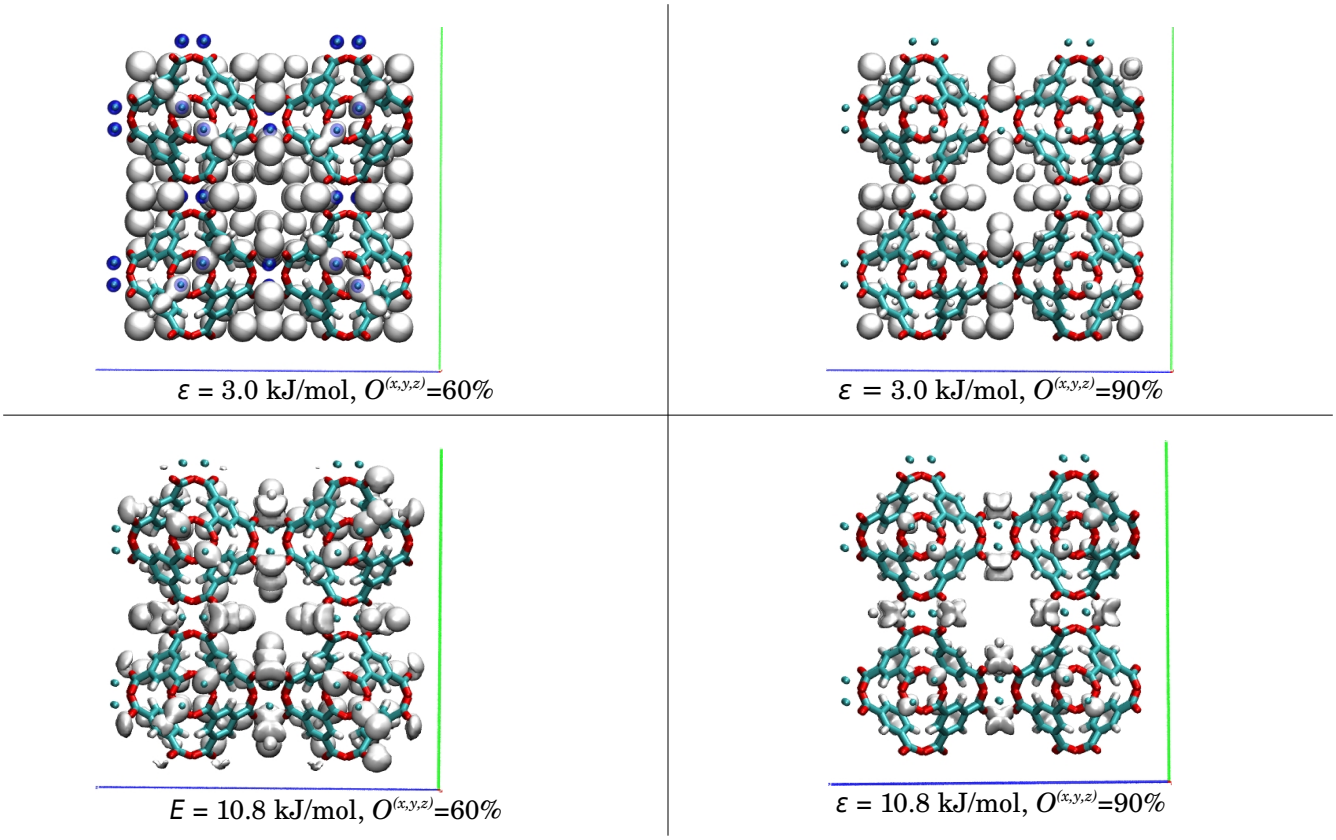

Figure S4. Occupancy maps calculated from MD simulations with a Morse function for the H_2···Cu(II) interaction employing different values of 'ε'.

The results obtained with the Morse function, showed in Figure S4, were better than the obtained with the LJ function. At lower values of $O^{(x,y,z)}$ (<60%) the occupancy maps provide us a clearer definition of the adsorption positions in the bigger cavities that the observed with the LJ function. Additionally, at lower values of occupancy it was possible to identify different adsorption positions into the smallest cavities of the HKUST-1, which according to the experimental results[1] are dependent of the loadings.

For comparison, the LJ and Morse potential functions with the relevant values of 'ε' (3.0 and 10.8 kJ/mol) employed in the parameterization are depicted in Figure S5. The interaction distance was fixed to the experimental result (2.5 Å)

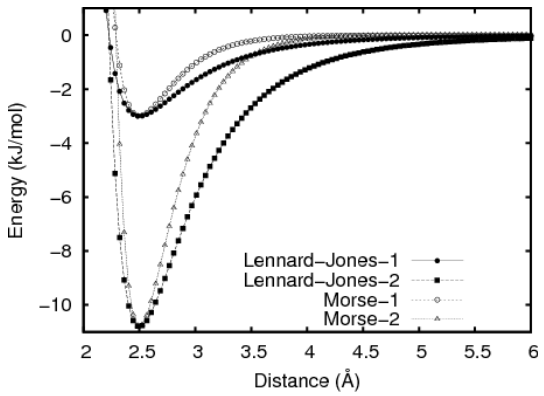

Figure S5. Comparison of the Lenard Jonnes (LJ) and Morse (α=3.0) potential functions for different well depths. 3.0 kJ/mol (1) and 10.8 kJ/mol (2).

S4. DFT calculations of H_2 adsorption in the Paddle wheel IBU.

The SSB-D functional comprises a modification to the exchange part of the original PBE functional in an attempt to recover in the same functional the good results of the PBE functional for weak interactions and the properties of OPBE functional for handling spin states in transition metal complexes[2]. Additionally, the Grimme's dispersion correction was added to enhance the quality of the results for weak interactions. Although the SSB-D functional has been successfully tested in systems in which the main weak interactions are hydrogen bondings and $\pi\cdots\pi$ staking, the good results obtained for these systems leaded us to test this functional in the dispersion driven interaction $H_2\cdots$Metal.

A deep evaluation of the accuracy of the functional for this interaction must be done by comparing the computed interaction energies with SSB-D and the results obtained with a more accurate quantum chemistry methodology. With this aim we have performed MP2 calculations, however, given the dependence of the MP2 calculations of the quality of the reference wave function (RHF, UHF or ORHF), we did not get successful results and a comparison of the SSB-D results was precluded.

Regarding to the case of the interaction $H_2\cdots$Cu-paddle wheel, as mentioned in the main manuscript, the results with PBE range from -5.8 kJ/mol for a cluster model of the paddle wheel to -13.4 kJ/mol for the same interaction in a periodic model of the MOF-505.

With the aim to obtain a more accurate estimation of the strength of the $H_2\cdots$Cu(II) interaction in the paddle wheel IBU and to define the maximum number of H_2 molecules that can be adsorbed in the IBU, we have performed DFT calculations employing the SSB-D functional with the def2-TZVP basis set. The density fitting approach was employed for the computation of the Coulomb potential.

As a first step, the cluster geometry was optimized at the B3LYP/def2-TZVP theoretical level with a singlet multiplicity and a starting C_{4h} symmetry. The final geometry kept the symmetry and was in excellent agreement with the experimental geometry reported in the crystallographic data for the different paddle wheel containing MOFs. As a further step, H_2 molecules were placed at different sites around the IBU an their coordinates were optimized at the SSB-D/def2-TZVP theoretical level.

The cluster model employed for the calculations and the adsorption positions for H_2 located around the paddle wheel IBU are presented in the Figure S6. The computed adsorption energies are summarized in Table S1.

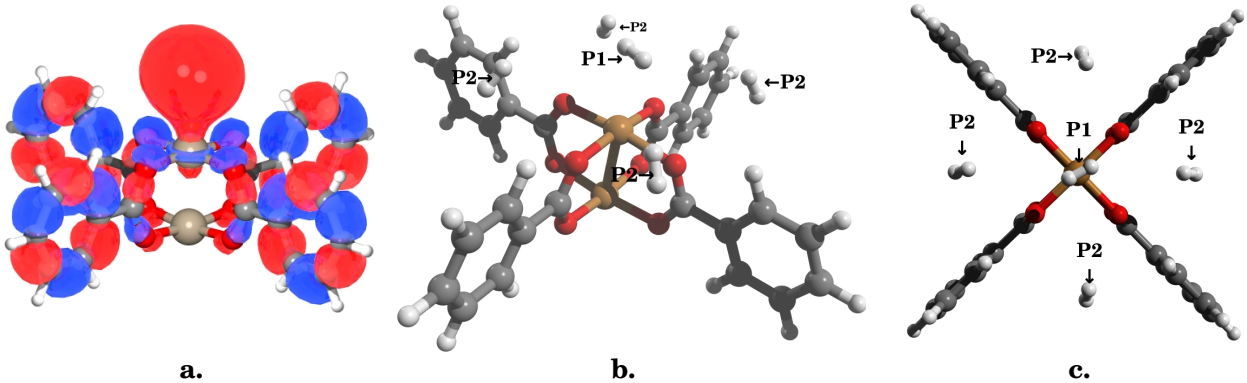

a. **b.** **c.**

Figure S6. a. Cu···H_2 orbital interaction. b. Horizontal and c. perpendicular views of the Paddle wheel IBU with 5 H_2 molecules located at the optimized positions obtained from the DFT calculations. Positions 1 (P1, strongest) and Positions 2 (P2, weaker) are indicated.

Table S1. Adsorption (E_{ads}) and BSSE corrected adsorption energies ($E_{ads\text{-}BSSE}$, kJ/mol) calculated at the SSB-D/def2-TZVP theoretical level for nH_2 molecules adsorbed at different positions (P1 and P2) of the Cu-paddle wheel model. Average adsorption energies ($E_{ads\text{-}BSSE}$/n) and relevant interactions distances (Å) are listed.

n (position)	1 (P1)	1 (P2)	2 (P1 + P2)	5 (P1 + P2)
E_{ads}	-11,3	-4,5	-15,2	-27,1
$E_{ads\text{-}BSSE}$	-10,8	-4,6	-14,6	-25,8
$E_{ads\text{-}BSSE}$/n	-10.8	-4,6	-7.3	-5.2
H_2···Cu	2.6	3,9	2.6/3.9	2.6/3.9
H_2···O	3,2	3,2	3,2	3,2

Two adsorption positions were identified around the paddle wheel IBU. The first one, labelled as P1 in Figure S6, corresponds to the strongest adsorption site located over the Cu(II) atoms at a distance of 2.6 Å, with and adsorption energy of -10.8 kJ/mol. This strong interaction is promoted by an small orbital interaction between the $\sigma_{H\text{-}H}$ orbital and the unoccupied d_{z2} and s orbitals of the Cu atoms as depicted in the Figure S6a and described in more detail by Kim et al[3].

The second adsorption position, P2, is placed between the carboxylate groups slightly located over the plane defined by the CuO_4 atoms at 3.9 Å of the Cu(II) atom (See Figure S6, b and c). The computed adsorption energy for this position was, -4.6 kJ/mol, a value significantly lower than the obtained in the strongest site.

The result with two H_2 molecules (n=2, Table S1) indicates a quite small effect of the simultaneous occupation of position P1 and P2 in the adsorption energies (with a repulsion energy 0.8 kJ/mol) and a no evident effect in the interaction distances. This fact and the topology of the IBU indicate that a total of five molecules could be adsorbed per metal atom. In order to confirm this estimation we carried out the calculation with five H2 molecules (n=5, see Table S1). As in the case when n=2, there is not a significant repulsion (3.4 kJ/mol) between the adsorbed molecules which confirm that at saturation the five adsorption positions located per metal atom can be occupied simultaneously.

Moreover, the average adsorption energy computed for five H_2 molecules reached a value (-5.2 kJ/mol) which is into the range of the experimental heats of adsorption reported for some paddle wheel containing MOFs (see Table 1).

S5. Adsorption positions in MOF-5, MOF-177 and cuboctahedral cavities.

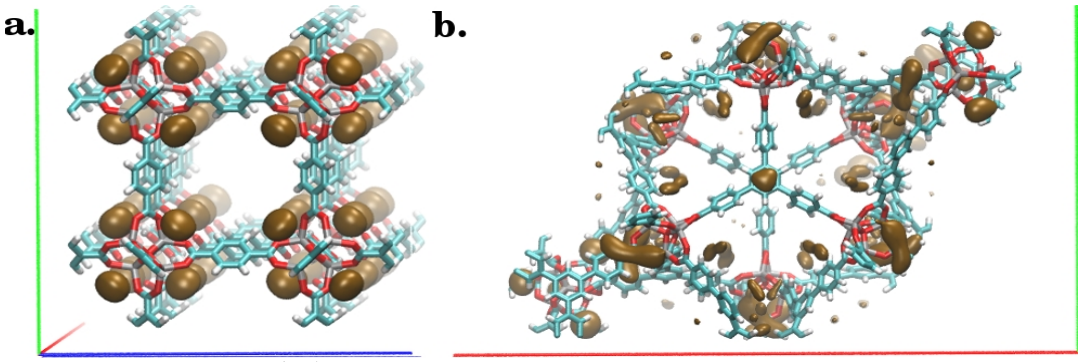

Figure S7. Occupancy maps ($O^{(x,y,z)}$<30%) for a. MOF-5 and b. MOF-177. Adsorption positions close to the IBUs and to the organic linkers in MOF-177 are observed.

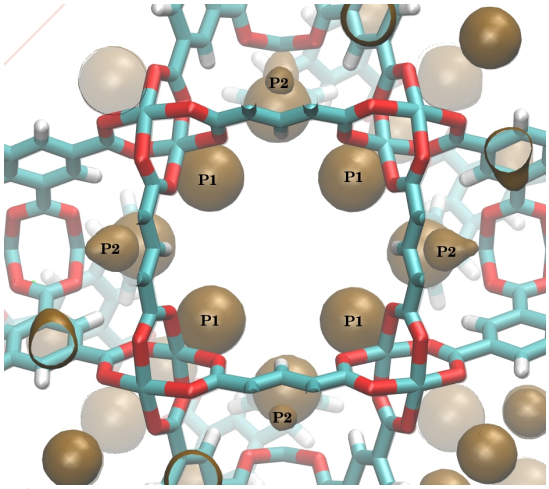

Figure S8. Occupancy map ($O^{(x,y,z)}$=80%) of cavity type V (cuboctahedral). The strongest adsorption positions (P1) and the enhanced-adsorption P2 positions at the narrow windows (containing 3 neighbour paddle wheels) are indicated.

S6. H_2 mobility as a function of the adsorption centre.

In order to gain insight on the mobility of the H_2 molecules adsorbed in the framework cavities (at 77 K) we drawn the trajectories for three molecules adsorbed at the identified adsorption positions P1, P2 and P3.

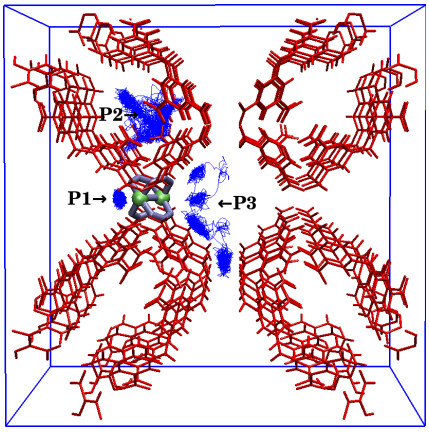

Figure S9. Trajectory (blue lines) followed by three H_2 molecules, adsorbed at the adsorption centres P1, P2 and P3 (see Figure S6), along the MD simulation at 77 K. The framework have been drawn in red and copper atoms were removed for clarity, one paddle wheel IBU have been highlighted.

The Figure Sx presents the trajectory followed for three molecules adsorbed at the identified adsorption positions. The graph suggest a very limited mobility of the molecule adsorbed at the strongest adsorption centre P1 where only rotation moves are observed. Conversely, from the trajectories followed by the molecules adsorbed at position P2 and P3 it is possible to observe hops between well defined adsorption centres.

The shape of the trajectory of the molecule adsorbed at position P2 is closely related with a window with three adjacent paddle wheel units. On the other hand, the trajectory of the molecule adsorbed at position P3 shows hops between positions P3 and P2 which are close in that particular cavity (cavity type I, Figure 6).

S7. Gravimetric uptakes as a function of m/ρ_{MOF}

Given that 'n' can be, obviously, considered the same for the same IBU, as it is the case for paddle-wheel containing MOFs; and considering that '$m \cdot n$'$<< \rho_{MOF}/3.343$, the equation 4 (main manuscript) can be rewritten as (assuming n=1):

$$wt\,\% = \frac{m \cdot n \cdot 3.343}{\rho_{MOF}\left(g/cm^3\right)} \cdot 100 \propto \frac{m}{\rho_{MOF}} \qquad \text{(S1)}$$

With the expression S1 it is possible to identify whether the experimental uptakes correlate with the calculated by plotting wt% vs m/ρ, where the latter values have been calculated from data in Table 4. A lack of correlation may indicate, we suggest, that the confinement effect -not taken into account to derive this equation- is playing a significant role in the observed uptakes.

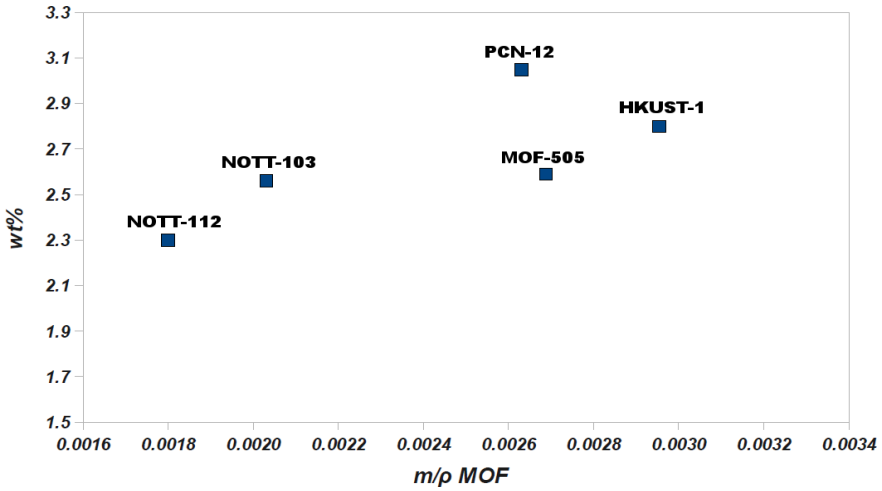

Figure S10. Experimental excess gravimetric uptake (wt%) as a function of 'm/ρ_{MOF}' according to the expression S1 for the paddle wheel containing MOFs.

Table S2. Proportionality between experimental uptakes (Table 3) and m/ρ_{MOF} according to equation S1.

MOF	Experimental wt%	m/ρ_{MOF}
PCN-12	3,05	0,0026
HKUST-1	2,80	0,0030
MOF-505	2,59	0,0027
NOTT-103	2,56	0,0020
NOTT-112	2,30	0,0018
MOF-5	1,32	0,0032
MOF-177	1,25	0,0021

S8. Adsorption Isotherm

In order to test the set of parameters, employed successfully in the location of the adsorption regions via Molecular Dynamic simulations, for the estimation of the H_2 uptake at higher pressures (> 1 bar), we performed GCMC simulations to compute the adsorption isotherm at 77 K. The result is presented in Figure S11.

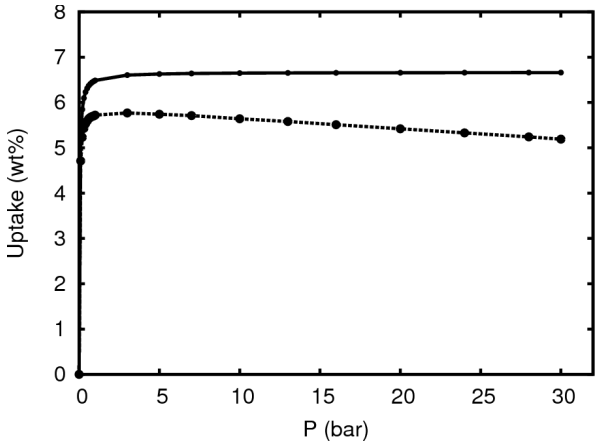

Figure S11. Hydrogen adsorption isotherm for HKUST-1 calculated at 77 K with the force field parameters listed in Table 2. Absolute (solid line) and Excess (dashed line) adsorption.

Despite the Cu···H_2 parameters were defined from the closely related experimental and theoretical (SSB-D/def2-TZVP) results, the shape of the computed isotherm indicates a stronger interaction of the adsorbate with the framework surface which induces an overestimation of the uptake as compared with the experimental or theoretical results[4].

Some of the factors which may explain this overestimation are: (i) neglect of the thermal corrections in the estimation of the interaction energy, (ii) neglect of the the framework flexibility in the GCMC simulations and (iii) absence of defects on the simulated surface with respect to the experimental sample.

Regarding to the Cu···H_2 interaction strength, it is worth to note that the adsorption energy of our potential is slightly stronger (-10.8 kJ/mol) than the reported experimentally (-10.1 kJ/mol)[5] for the strongest adsorption centre. Employing a similar approach for the parameterization, Fischer et al.[4] reported an isotherm calculated with a weaker interaction potential (-5.8 kJ/mol), which was in excellent agreement with the experimental results at low pressures. However at high pressures the uptake was overestimated. Conversely, the isotherm computed with the UFF force field, which presents a significantly weaker Cu···H_2 interaction (-0.3 kJ/mol), was closer to the experimental at high pressures. This suggests that additional effects to the interaction with the metal centres are playing an important role in the adsorption at high pressures.

1 V. K. Peterson, C. M. Brown, Y. Liu, and C. J. Kepert, *Science And Technology*, 2011, 0-6.

2 M. Swart, M. Solà, and F. M. Bickelhaupt, *The Journal of chemical physics*, 2009, 131, 094103.

3 Y.-H. Kim, J. Kang, and S.-H. Wei, *Physical Review Letters*, 2010, 105, 1-4.

4 M. Fischer, B. Kuchta, L. Firlej, F. Hoffmann, and M. Fröba, *The Journal of Physical Chemistry C*, 2010, 353–358.

5 J. G. Vitillo, L. Regli, S. Chavan, G. Ricchiardi, G. Spoto, P. D. C. Dietzel, S. Bordiga, and A. Zecchina, *Journal of the American Chemical Society*, 2008, 130, 8386-96.